



# Microbubbles with surface coated by superparamagnetic iron oxide nanoparticles

Wen He<sup>a</sup>, Fang Yang<sup>a</sup>, Yihang Wu<sup>a</sup>, Song Wen<sup>b</sup>, Ping Chen<sup>a</sup>, Yu Zhang<sup>a</sup>, Ning Gu<sup>a,\*</sup>

<sup>a</sup> State Key Laboratory of Bioelectronics and Jiangsu Laboratory for Biomaterials and Devices, Southeast University, Nanjing 210096, China

<sup>b</sup> Department of Radiology, Zhong Da Hospital, School of Clinical Medicine, Southeast University, Nanjing 210009, China

## ARTICLE INFO

### Article history:

Received 17 March 2011

Accepted 5 October 2011

Available online 12 October 2011

### Keywords:

Microbubbles

Nanoparticles

Composite materials

Multilayer structure

Ultrasound imaging

Magnetic resonance imaging

## ABSTRACT

Microbubbles (MBs) with the ability of enhancing ultrasound image contrast and delivering drugs are widely used in medical applications. By combining microbubbles and superparamagnetic iron oxide (SPIO) nanoparticles, dual-modality contrast agent for both ultrasound and magnetic resonance (MR) imaging can be obtained. In this study, we synthesized microbubbles with a novel structure, which included a nitrogen gas core, a polymer shell, and SPIO nanoparticles on the shell surfaces. In vitro experiments showed that microbubbles with such structure provided both higher ultrasound and MR enhancement than blank microbubbles without SPIO nanoparticles and previously designed SPIO-embedded microbubbles. Furthermore because SPIO-coated microbubbles have abundant amino groups on the surface, such microbubbles have potentiality for targeted imaging after specific targeted ligands or antibodies are linked.

© 2011 Elsevier B.V. All rights reserved.

## 1. Introduction

Ultrasound medical imaging is widely used for clinical diagnosis purpose, but the imaging has low resolution without the help of contrast agents. During the past several decades, gas-filled microbubbles represent the most efficient ultrasound contrast agents (UCAs). Under diagnostic image guidance, the microbubbles (MBs) also can be used as drug delivery vehicles due to the fact that under proper ultrasound pressures microbubbles can rupture and release drugs, so drugs can be precisely delivered to the appointed regions. Such ultrasound mediated drug delivery performs the least invasive therapy [1].

Polymer-shelled microbubbles are preferable for many therapeutic applications, because they have higher stability in circulation, thicker shells into which drugs can be incorporated, and the pressure thresholds for acoustic destruction of which can be controlled by changing polymer's molecular weight, crystallinity, hydrophobicity etc. [1–3]. When the polymer shells are incorporated with other agents, the back-scattering signals will accordingly change. For example, E. Stride et al. proved that after depositing gold nanoparticles on the surface of microbubbles, the nonlinear response was improved at low pressures [4], which is a beneficial factor for US imaging. Nowadays SPIO nanoparticles are commonly used as negative contrast agents of MR imaging, for they can shorten the transverse relaxation time ( $T_2$ ) of water protons [5]. In previous work, we have synthesized microbubbles as dual contrast agents for ultrasound and MR imaging by embedding SPIO

nanoparticles into polymeric shells [6]. However, R. Kaiser and G. Miskolcay demonstrated that the magnetic properties of colloidal magnetite ferrofluids could be affected by nonmagnetic surface layer [7]. So we predict microbubbles with SPIO nanoparticles on surfaces may retain magnetic property better, thus better for  $T_2$ -weighted MRI enhancement.

The goal of this study was to improve the dual-modality contrast agents, so we modified the synthesis procedure. Firstly PVA was oxidized by periodate and chlorite [8], which was called telechelic PVA with carboxylic groups at chains' ends. And then, MBs were fabricated using telechelic PVA, after that, SPIO nanoparticles with amino group coatings were linked to microbubbles' surfaces by chemical reaction. In vitro experiments were taken to test the ability for US and MRI enhancement. Besides, nanoparticles on surfaces could directly interact with surrounding cells and tissues, after microbubbles rupture, may stay in the region for further medical application.

## 2. Materials and methods

### 2.1. Materials

Aminopropyltriethoxysilane (APTS) coated SPIO  $\gamma$ -Fe<sub>2</sub>O<sub>3</sub> (ATPS/ $\gamma$ -Fe<sub>2</sub>O<sub>3</sub>) nanoparticles were provided by Jiangsu Key Laboratory for Biomaterials and Devices [9]. Poly (vinyl alcohol) (PVA) ( $M_w = 31,000$ ) was from Sigma-Aldrich; poly (L-lactide) (PLLA) ( $M_w = 15,000$ ) was from Shandong Daigang company. Sodium periodate and sodium chlorite were purchased from Shantou Xilong Chemical company. 1-Ethyl-3-(3-dimethylaminopropyl) carbodiimide (EDC) and 2-(N-morpholino) ethanesulfonic acid (MES) were from Shanghai Medpep company. Span 80, Tween 80 and N<sub>2</sub> were reagent grade.

\* Corresponding author. Tel./fax: +86 25 83272476.

E-mail address: [guning@seu.edu.cn](mailto:guning@seu.edu.cn) (N. Gu).

## 2.2. Fabrication of SPIO-coated microbubbles

The telechelic PVA was firstly synthesized as Gaio Paradossi et al. described method [10]. The microcapsule fabrication and separation methods were described in our previous paper [6]. The difference was using telechelic PVA solution instead of original PVA solution and not adding SPIO nanoparticles into methylene chloride solution.

After separated from free telechelic PVA, microcapsules were suspended in MES buffer (50 mM, pH = 5.4). The suspension was activated by EDC (0.4 mg/ml) at room temperature, and then incubated with a certain amount of ATPS coated SPIO  $\gamma$ -Fe<sub>2</sub>O<sub>3</sub> nanoparticles. After 48 h, products were collected and washed 3 times by distilled water. Products were stored in vials and lyophilized (FreeZone freeze dryer, LABCONCO, USA) using mannitol as a protective agent. After drying cycle was completed, N<sub>2</sub> was introduced into vials.

## 2.3. Fabrication of SPIO-embedded microbubbles and blank microbubbles

The same nanoparticles were used to fabricate SPIO-embedded microbubbles. The fabrication method was similar to that described in previous paper [6], just not adding nanoparticles into methylene chloride, but adding nanoparticles into PVA aqueous solution. Blank microbubbles were synthesized using the same method without adding SPIO nanoparticles.

## 2.4. Characterization

The morphology and structure were studied by scanning electron microscope (SEM) and transmission electron microscope (TEM).

Magnetization properties were studied by vibrating sample magnetometer (VSM) after the samples were dried at 70 °C.

## 2.5. In vitro acoustic imaging experiments

In vitro acoustic imaging experiments were performed in a self-made phantom. Samples were tested and imaged by a digital B-mode diagnostic ultrasonic instrument Belson 3000A (Belson Imaging Technology Co., Ltd, Wuxi, China) with a 3.5 MHz R60 convex array probe.

Software based on Microsoft Visual C++ 6.0 (Microsoft, USA) was developed to quantitatively measure the mean gray scale values of ultrasound images. When a region of interest (ROI) was selected, the mean gray scale value of ROI was calculated automatically.

All microbubbles samples were prepared using the same centrifugation isolation method, and concentrations were  $1.8\text{--}1.9 \times 10^8$  MBs/ml. For microbubbles containing SPIO nanoparticles, the iron concentration was 91.73  $\mu\text{g/ml}$ . Such samples were also used for MRI testing.

## 2.6. In vitro MRI experiments

MRI was performed on 7.0 T Micro-MRI (PharmaScan, Bruker, Germany). To obtain absolute T<sub>2</sub> relaxation time values, multi-slice multi-echo (MSME) T<sub>2</sub> map sequence was used. The detailed scan parameters are: TR 3000 ms, TE 12 ms to 192 ms in steps of 12 ms, field of view (FOV) 60 × 60 mm, matrix size 256 × 256, slice thickness 1 mm, 1 slice, number of average 1, total scan 8 min. T<sub>2</sub> relaxation time was calculated by paraVision 5.0 post-processing software.

Two types of samples were tested, including suspensions of SPIO-embedded microbubbles and SPIO-coated microbubbles. The

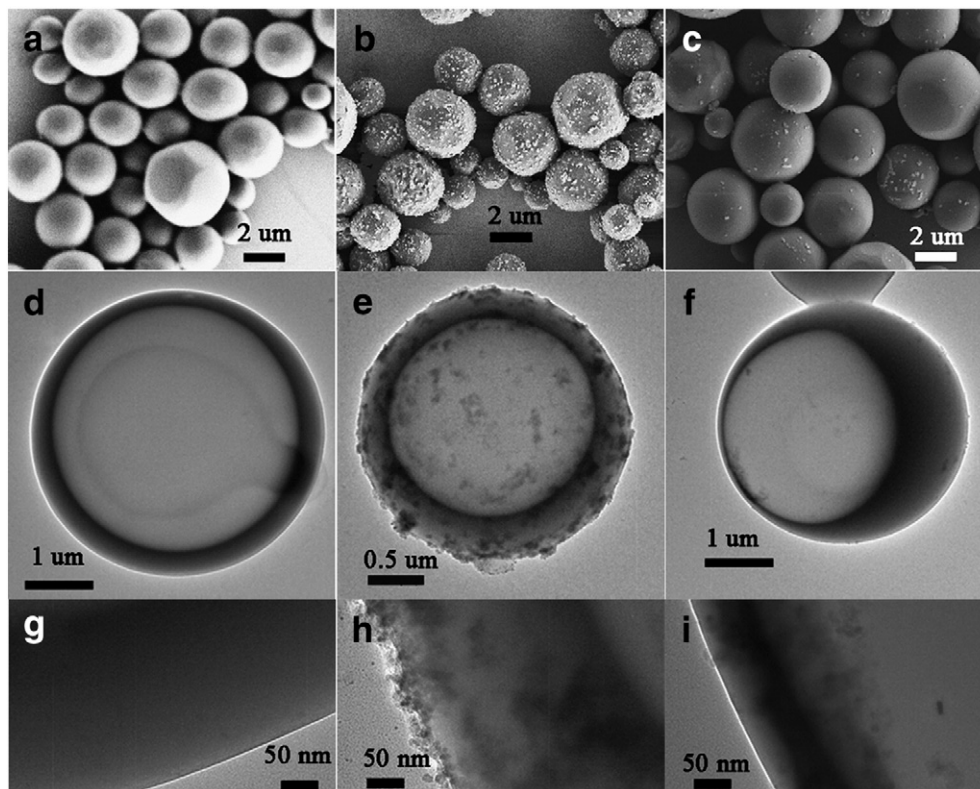


**Fig. 1.** SEM images of (a) blank microbubbles, (b) SPIO-coated microbubbles, (c) SPIO-embedded microbubbles, TEM images of (d) blank microbubble, (e) SPIO-coated microbubble, (f) SPIO-embedded microbubble, (g–i) are partially enlarged images of (d–f).

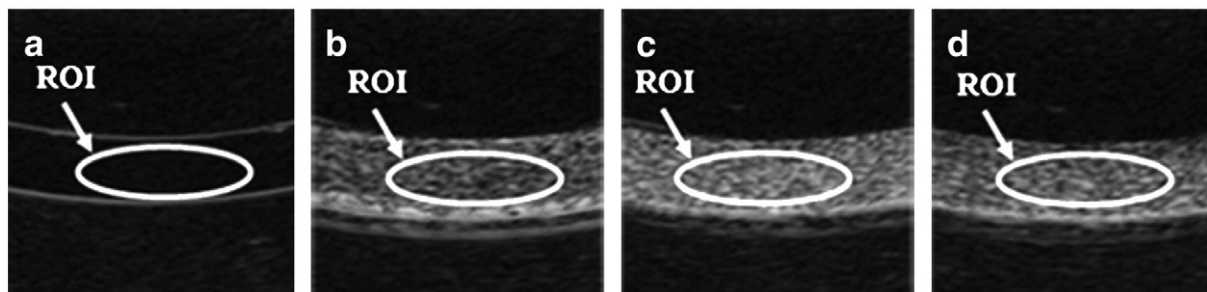


Fig. 2. B-mode ultrasound images of (a) distilled water, (b) blank microbubbles, (c) SPIO-coated microbubbles and (d) SPIO-embedded microbubbles.

suspensions were then diluted to different volume fractions from 100% to 10% by adding distilled water.

### 3. Results and discussion

#### 3.1. Characterizations

Fig. 1 is the SEM and TEM characterization of microbubbles. SEM images showed that all microbubbles were spherical. Blank microbubbles' surfaces were smoothest, SPIO-embedded microbubbles' surfaces were coarser and SPIO-coated microbubbles' surfaces were coarsest. TEM images showed the distributions of nanoparticles. No nanoparticles could be observed from blank microbubble. On SPIO-coated microbubble's surface nanoparticles were randomly distributed, but for SPIO-embedded microbubble, nanoparticles were mostly distributed within the shell, only a few were adsorbed on surface (Fig. 1h and 1i).

#### 3.2. In vitro acoustic testing

The B-mode ultrasound images shown in Fig. 2, which indicates that SPIO-coated and SPIO-embedded microbubbles have higher mean gray scale values ( $116.12 \pm 4.09$  and  $102.46 \pm 4.09$ ) than blank microbubbles ( $74.02 \pm 4.47$ ). The reason may be that the nonlinear character of microbubbles was significantly increased by depositing

nanoparticles on microbubbles' surfaces without increasing the excitation, which is proved by the results of E. Stride, et al. [4].

The results also show that the SPIO-coated microbubbles have the highest ultrasound enhancement. From Fig. 1, nanoparticles were mostly distributed within the shell for SPIO-embedded microbubble, which may restrict the microbubble compression and reduce the rate of diffusion of the gas. However, the deposition of nanoparticles on the surface of the microbubbles for SPIO-coated microbubbles could make the shell of microbubbles have better viscoelastic property [11]. Then under the ultrasound exposure, nanoparticles on the surface may have more free degree than those embedded in shells, thus have less effect on preventing microbubble vibration. Besides, the randomly distributed nanoparticles on the shell surface can be responsible for the increase of the nonlinear behavior of the microbubble [12], which causes higher US imaging enhancement.

#### 3.3. In vitro MRI testing

The  $T_2$ -weighted images and transverse relaxation rates ( $R_2$ ) of SPIO-embedded microbubbles (I) and SPIO-coated microbubbles (II) with different volume fraction were shown in Fig. 3a and 3b. Approximately linear relationships were observed for both (I) and (II). It can be also observed that (II) had a steeper slope and a higher  $R_2$  value at each volume fraction. A possible explanation might come from the fact that SPIO nanoparticles on the surface directly exposed to magnetic

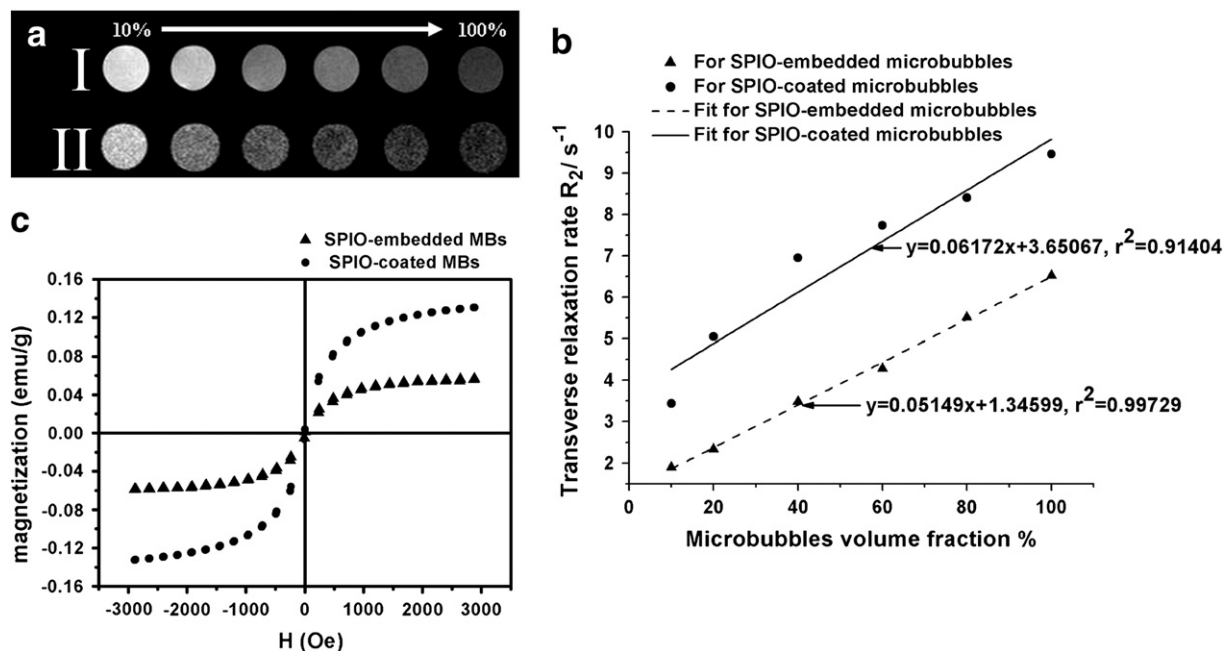


Fig. 3. (a) MR images of SPIO-embedded microbubbles (I), SPIO-coated microbubbles (II); relationship between  $R_2$  and volume fraction of two types of microbubbles (b), and (c) hysteresis loops of (I) and (II).

fields preserved better superparamagnetic properties than those embedded in polymeric shells, thus had a greater effect on alternating  $R_2$  value of surrounded water proton.

In order to verify the hypothesis, magnetic properties were studied by testing the hysteresis loops. The results indicated that both SPIO-coated and SPIO-embedded microbubbles preserved superparamagnetic properties. Besides, SPIO-coated microbubbles had a much higher saturated magnetization than SPIO-embedded microbubbles with the same SPIO concentration (Fig. 3c). As a control, VSM curve of microbubbles without SPIO nanoparticles cannot be obtained.

#### 4. Conclusion

In this study, we fabricated a novel multilayer emulsion microbubbles structure with SPIO nanoparticles on surfaces. Compared with previously synthesized SPIO-embedded microbubbles, SPIO-coated microbubbles provided both higher ultrasound and MR  $T_2$ -weighed contrast enhancement. However, it's important to note that the MRI enhancing ability strongly depends on SPIO nanoparticles' types, sizes, concentration, etc. In this study we just proved that with the same type, size, and amount of nanoparticles, SPIO-coated microbubbles preserve magnetic properties better than SPIO-embedded microbubbles. Furthermore nanoparticles on surfaces might directly interact with surrounding substance. So we predict SPIO-coated microbubbles will have a better clinical application.

#### Acknowledgments

The authors acknowledge the financial support from National Important Science Research Program of China (Nos. 2006CB705602, 2011CB933500), National Natural Science Foundation of China (Nos. 60725101, 50872021, 31000453), and Research Fund of Young Teachers for the Doctoral Program of Higher Education of China (Nos. 20100092120038).

#### References

- [1] Bohmer MR, Klivanov AL, Tiemann K, Hall CS, Gruell H, Steinbach OC. *Eur J Radiol* 2009;70:242–12.
- [2] Chlon C, Guedon C, Verhaagen B, Shi WT, Hall CS, Lub J, et al. *Biomacromolecules* 2009;10:1025–7.
- [3] Stride E, Edirisinghe M. *Soft Matter* 2008;4:2350–10.
- [4] Stride E, Pancholi K, Edirisinghe MJ, Samarasinghe S. *J R Soc Interface* 2008;5: 807–5.
- [5] Gould P. *Nanotoday* 2006;1(4):34–6.
- [6] Yang F, Li Y, Chen Z, Zhang Y, Wu J, Gu N. *Biomaterials* 2009;30:3882–9.
- [7] Kaiser R, Miskolczy G. *J Appl Phys* 1970;41(3):1064–9.
- [8] Barretta P, Bordi F, Rinaldi C, Paradossi G. *J Phys Chem B* 2000;104:11019–8.
- [9] Ma M, Zhang Y, Yu W, Shen H, Zhang H, Gu N. *Colloids Surf A Physicochem Eng Asp* 2003;212:219–8.
- [10] Paradossi G, Cavalieri F, Chiessi E, Ponassi V, Martorana V. *Biomacromolecules* 2002;3:1255–8.
- [11] Abkarian M, Subramaniam AB, Kim SH, Larsen RJ, Yang SM, Stone HA. *Phys Rev Lett* 2007;99:188301–1–4.
- [12] Sassaroli E, Li K, O'Neill B. *J Acoust Soc Am* 2009;126:2802–13.